SUPPORTING INFORMATION

Mesoporous amorphous FeOF nanococoons for high-rate and long-life rechargeable sodium-ion batteries

Shi Yan Fu,[a] Yuan Zhi Li, [a, b] Wei Chu,*[c] Yi Mei Yang, [a] Dong Ge Tong *[a] and Qing Le Zeng *[a]

[a] Mineral Resources Chemistry Key Laboratory of Sichuan Higher Education Institutions, College of Materials and Chemistry & Chemical Engineering, Chengdu University of Technology, Chengdu 610059, China. E-mail: tongdongge@163.com; qinglezeng@hotmail.com. Fax: +86 28 8407 9074

[b] Institute of Coal Chemistry, Chinese Academy of Sciences, Taiyuan 030001, China

[c] College of Chemical Engineering and Key Laboratory of Green Chemistry & Technology of Ministry of Education, Sichuan University, Chengdu 610065, China. E-mail: chuwei1965@foxmail.com; Fax: +86 28 8540 3397

Summary: 30 Pages; 2 Tables; 29 Figures

Table S1 Fitted EIS parameters of the as-prepared mesoporous amorphous FeOF nanococoons with different electrolytes at different temperatures.

Electrolytes	R_s / Ω					R_{ct} / Ω				
	298.15K	303.15K	308.13K	313.15K	318.15K	298.15K	303.15K	308.13K	313.15K	318.15K
NaTFSA/TGM	2.4	2.1	1.8	1.4	1.0	50.0	43.2	37.4	32.6	28.6
$NaPF_6$/TGM	2.3	2.1	1.9	1.6	1.2	80.1	66.7	56.0	47.2	40.1
$NaClO_4$/TGM	2.7	2.4	2.0	1.7	1.3	100.0	82.1	67.9	56.5	47.2
NaTFSA/EC-DEC	2.6	2.1	1.8	1.4	1.0	130.2	104.2	84.1	68.4	56.0
NaTFSA/PC	3.1	2.6	2.2	1.6	1.1	160.3	125.2	98.9	78.6	63.1
$NaPF_6$/EC-DEC	2.8	2.4	2.1	1.7	1.3	210.2	158.6	120.9	93.0	72.2
$NaClO_4$/PC	2.7	2.4	2.1	1.6	1.2	260.1	191.4	142.4	107	81.1

Table S2 Fitted EIS parameters of amorphous FeOF charging at 3.8 V at the 200th charging process with 1.0 M NaTFSA/TGM at 298.15 K.

	Conventional	Mesoporous nanococoons
R_s / Ω	5.9	2.6
R_{ct} / Ω	121.8	51.2
Warburg coefficient / $s^{1/2}cm^{-1}$	8.9×10^7	1.13×10^7

R_s represents for the electrolyte resistance, and R_{ct} for the charge transfer impedance.

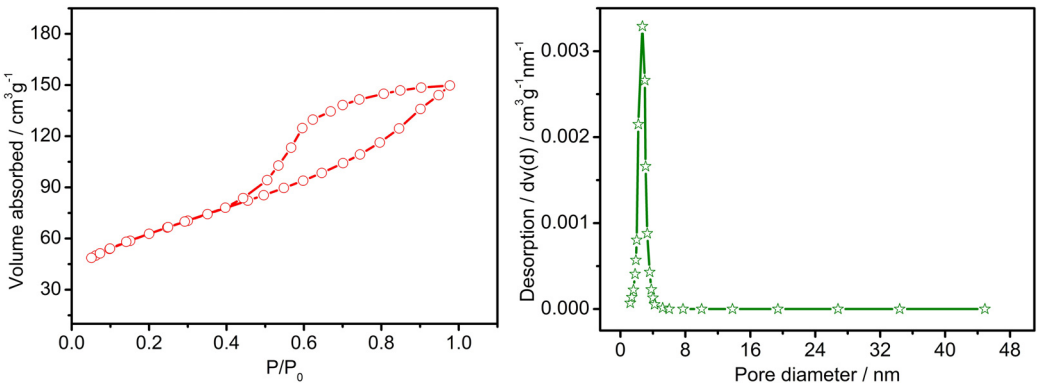

(a) (b)

Fig.S1 (a) N_2 adsorption–desorption plots and (b) pore size distribution of the as-prepared mesoporous amorphous FeOF nanococoons.

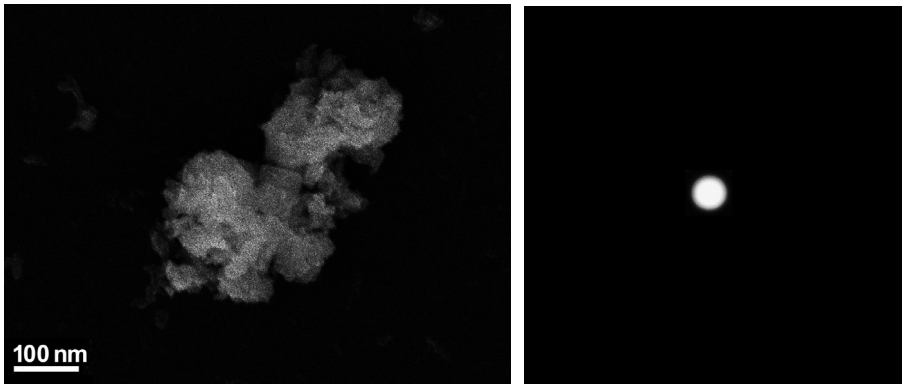

(a) (b)

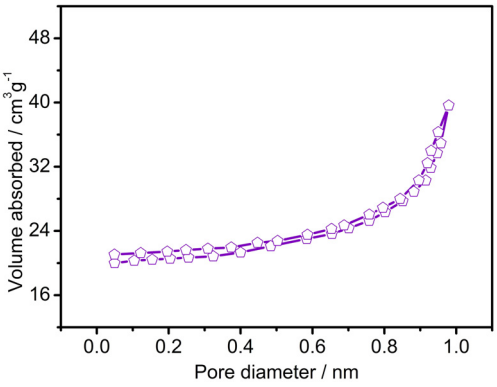

(c)

Fig.S2 (a) The typical STEM image, (b) SAED pattern and (c) N_2 adsorption–desorption plots of conventional amorphous FeOF.

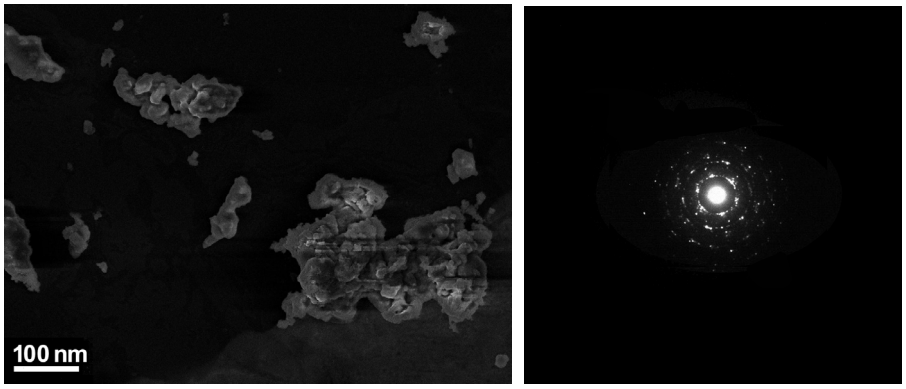

(a) (b)

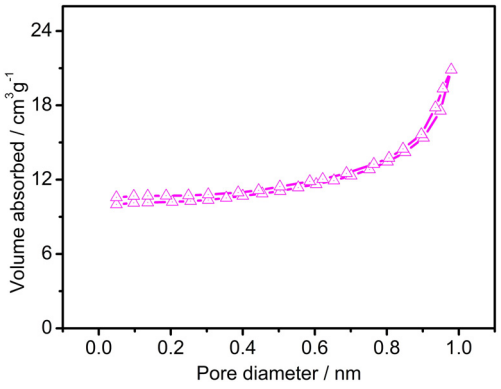

(c)

Fig.S3 (a) The typical STEM image, (b) SAED pattern and (c) N_2 adsorption–desorption plots of conventional FeOF crystalline.

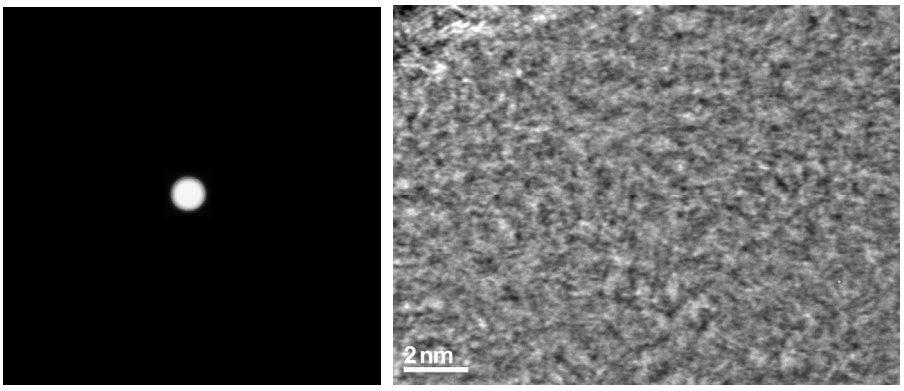

(a) (b)

Fig.S4 (a) SAED pattern and (b) HR-STEM of the as-prepared mesoporous amorphous FeOF nanococoons.

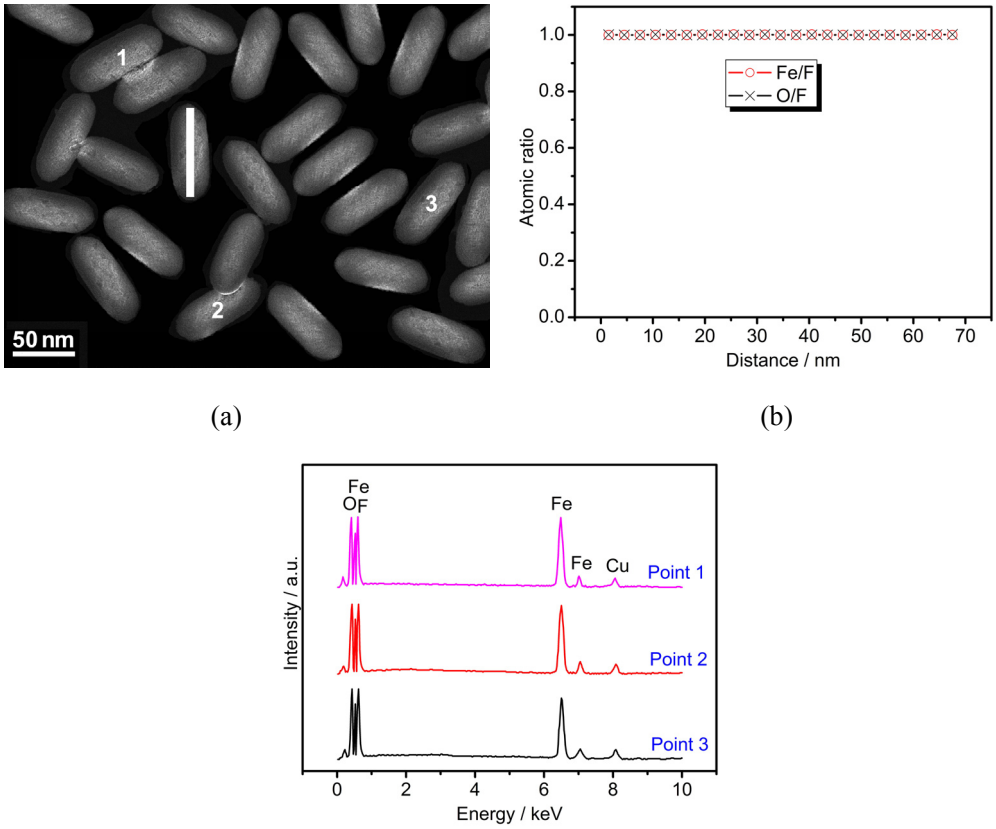

Fig.S5 (a) The high-angle annular dark-field scanning transmission electron microscopy (HAADF-STEM); (b) Fe/F and O/F atomic ratios recorded along the white cross-sectional compositional line shown in (a); (c) the Energy-dispersive X-ray spectroscopy (EDS) at points 1-3 in (a) of the as-prepared mesoporous amorphous FeOF nanococoons.

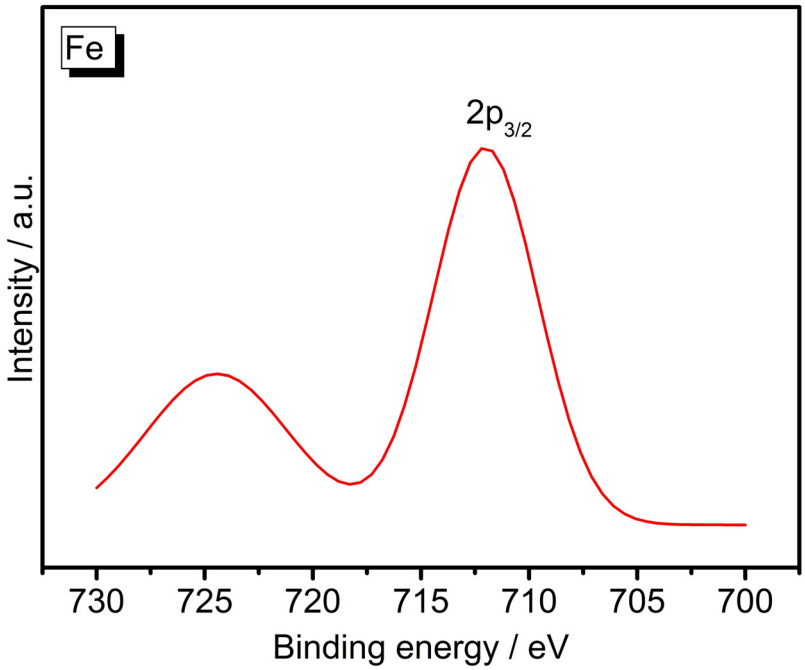

Fig.S6 Fe $2p_{3/2}$ XPS spectrum of the as-prepared mesoporous amorphous FeOF nanococoons.

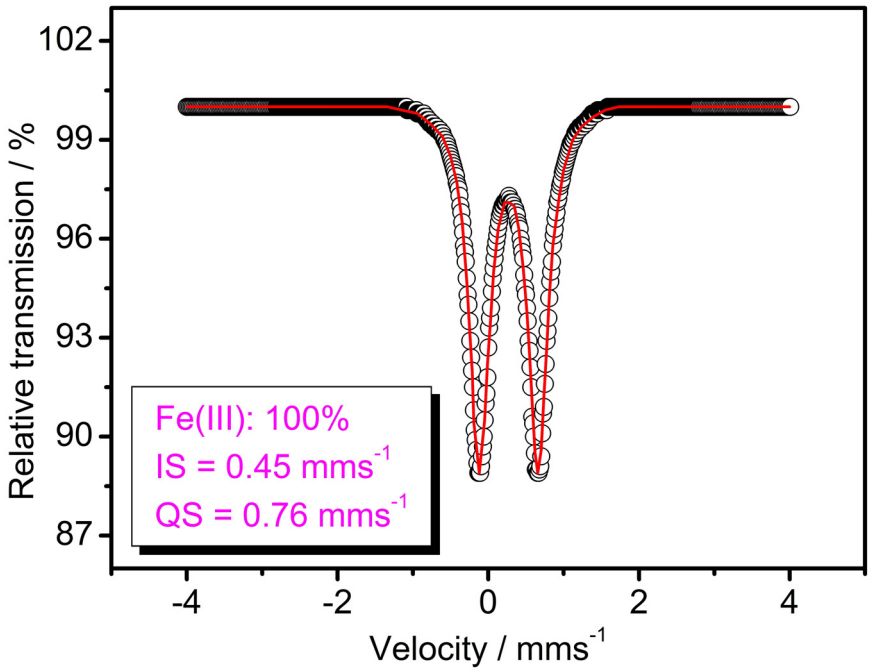

Fig.S7 Mössbauer spectrum of the as-prepared mesoporous amorphous FeOF nanococoons.

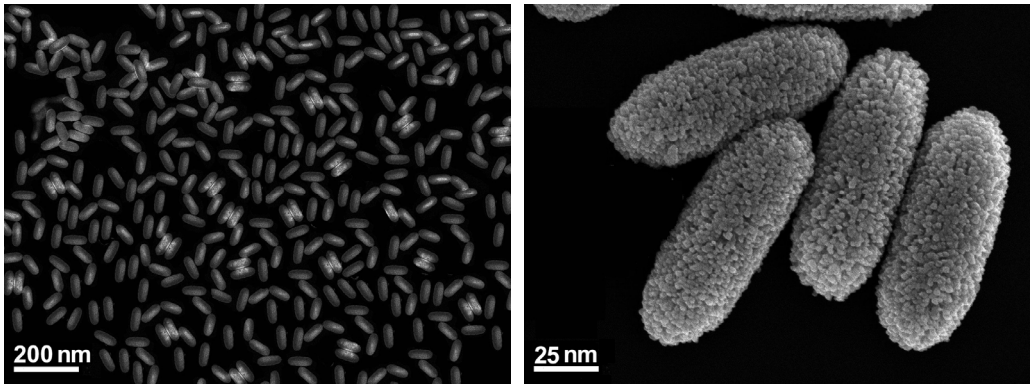

(a) (b)

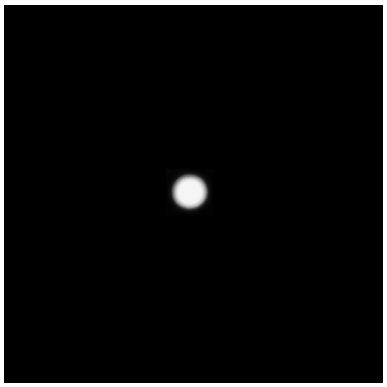

(c)

Fig.S8 (a) Low magnification STEM image, (b) enlarged STEM image and (c) SAED pattern of the as-prepared mesoporous amorphous FeOF nanococoons after sonication for 2 h dispersed in ethanol.

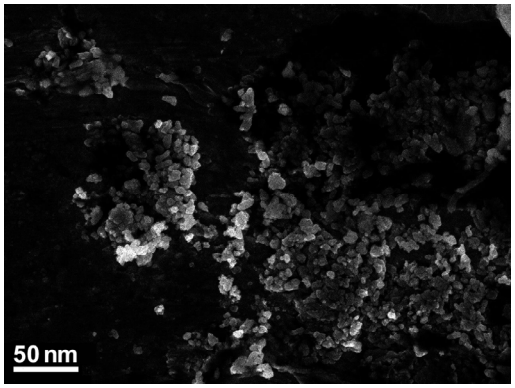

(a)

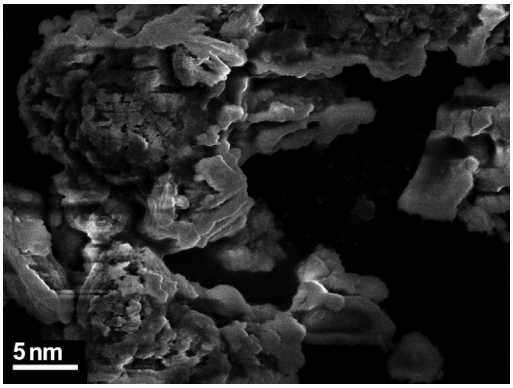

(b)

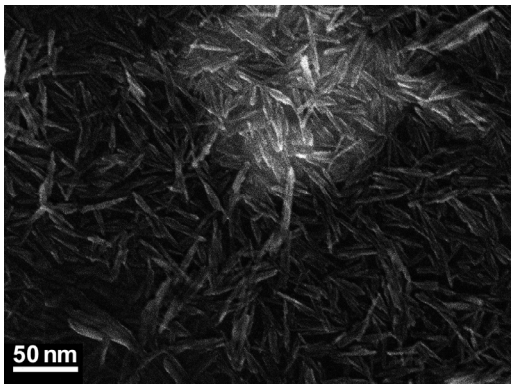

(c)

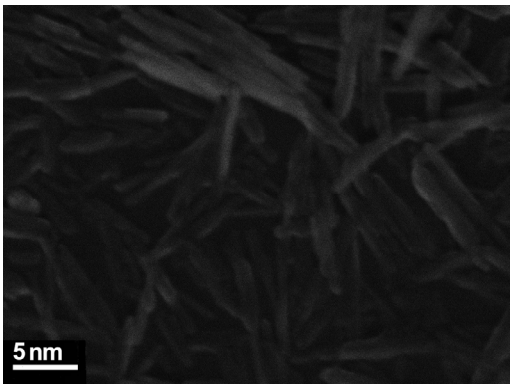

(d)

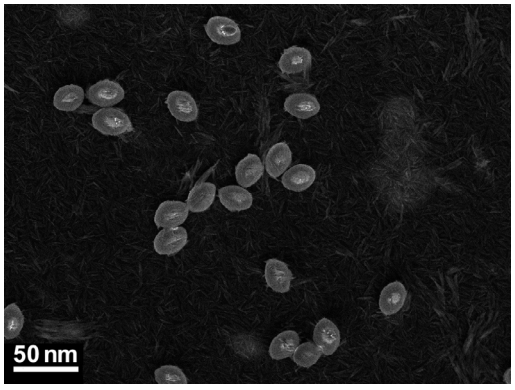

(e)

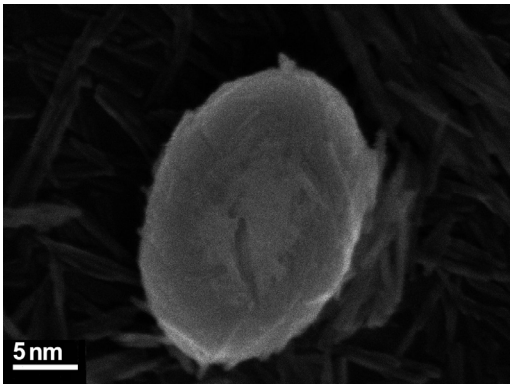

(f)

(Continued)

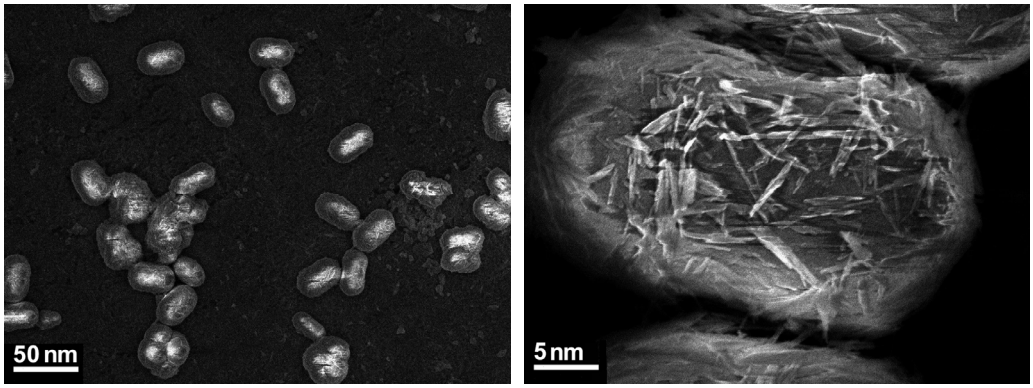

(g) (h)

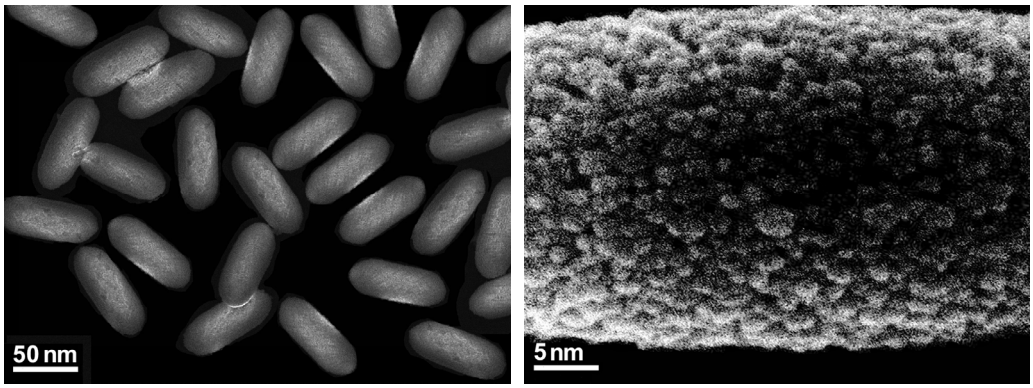

(i) (j)

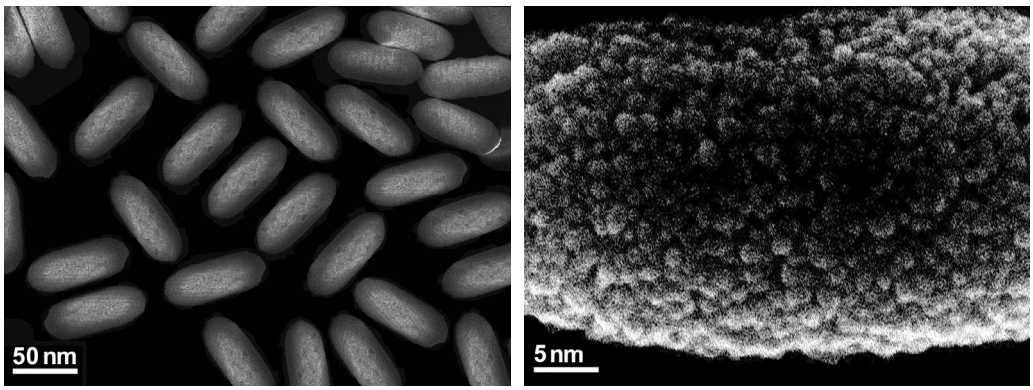

(k) (l)

Fig.S9 The Low magnification STEM and enlarged STEM images of the mesoporous amorphous FeOF nanococoons prepared via SPP for different times: (a) and (b) 0.5 min; (c) and (d) 1 min; (e) and (f) 2 min; (g) and (h) 5 min; (i) and (j) 10 min; (k) and (l) 30 min.

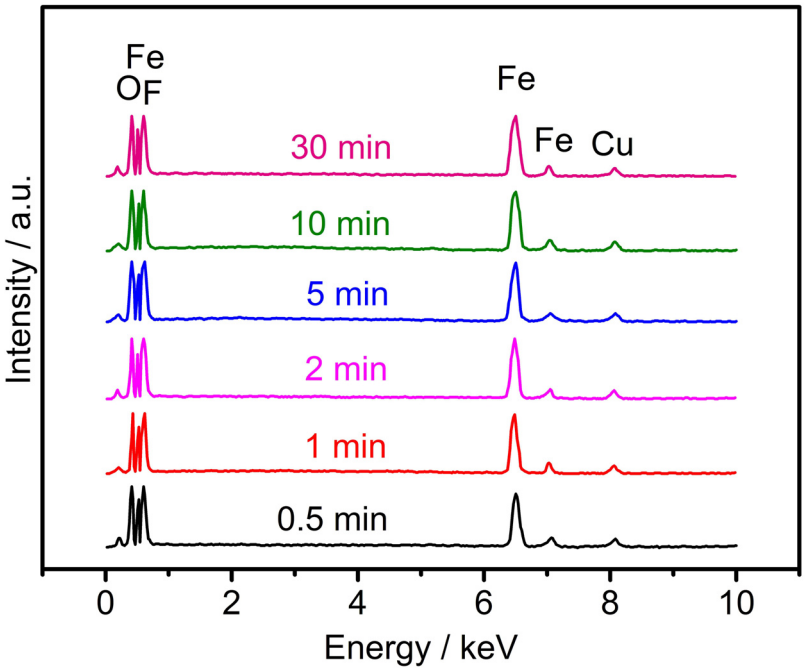

Fig.S10 Energy-dispersive X-ray spectroscopy (EDS) of the mesoporous amorphous FeOF nanococoons prepared with different reaction times.

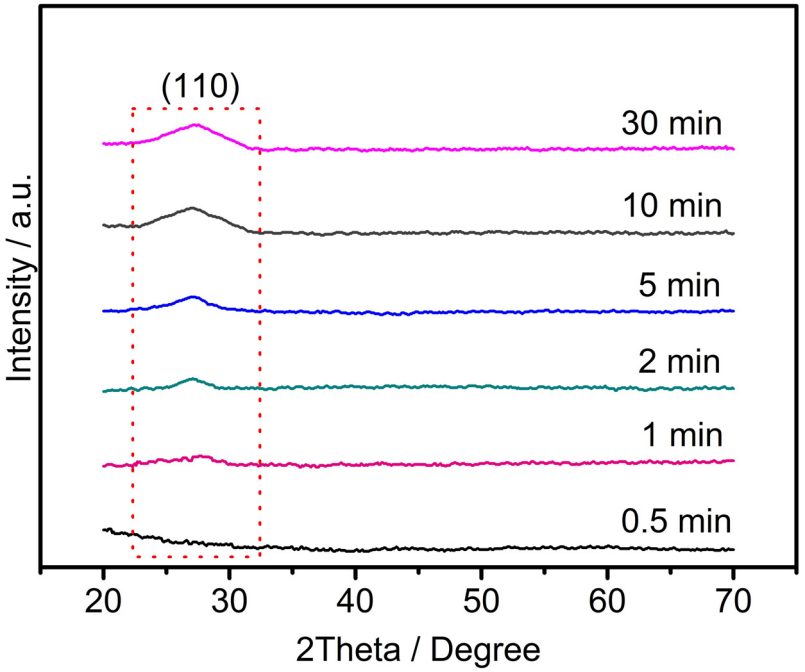

Fig.S11 XRD patterns of the mesoporous amorphous FeOF nanococoons prepared with different reaction times.

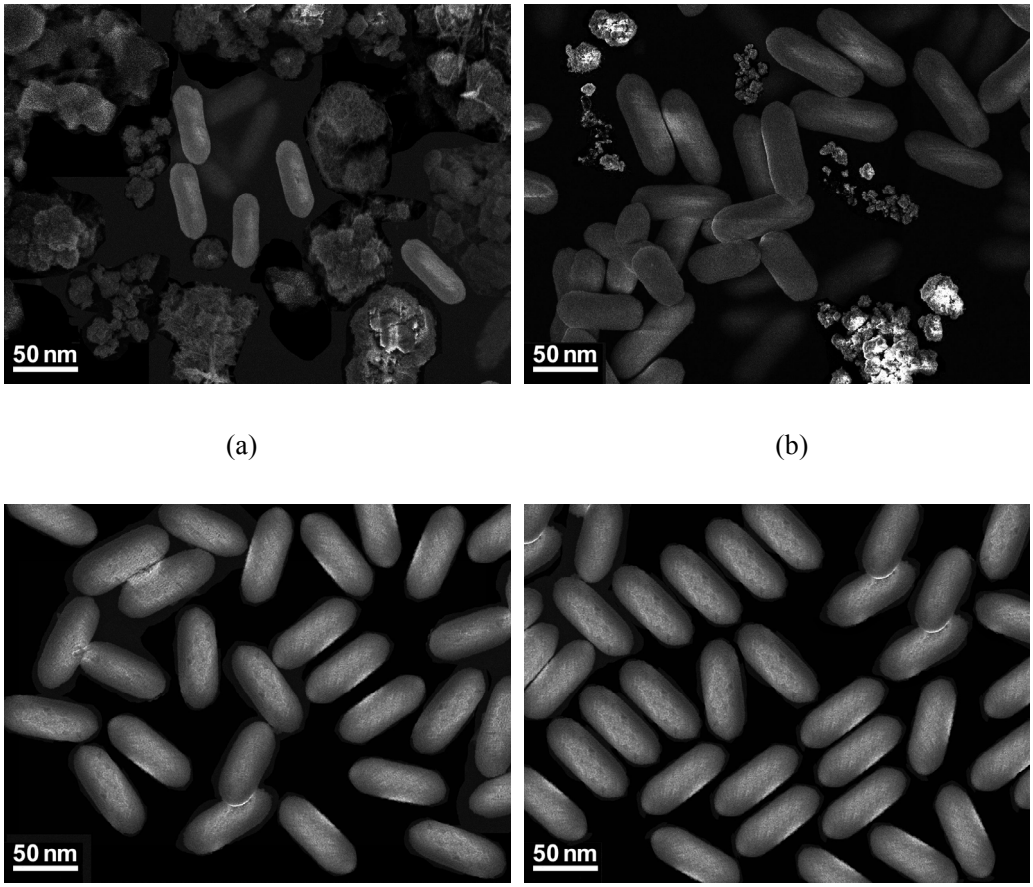

Fig.S12 STEM images of the as-prepared mesoporous amorphous FeOF nanococoons obtained with different amounts of $CO(NH_2)_2$: (a) 3 mmol, (b) 7 mmol, (c) 10 mmol, (d) 30 mmol.

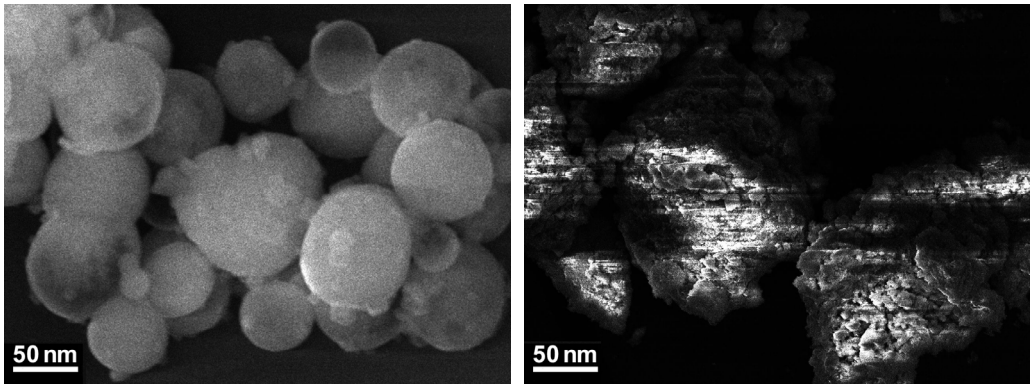

(a) (b)

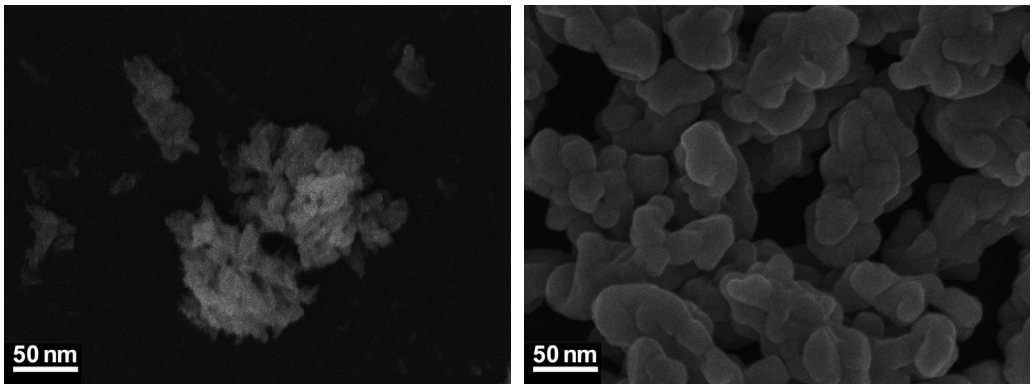

(c) (d)

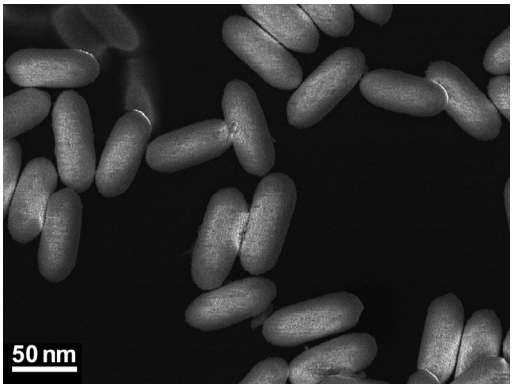

(e)

Fig.S13 STEM images of the as-prepared mesoporous amorphous FeOF nanococoons prepared via SPP with (a) OA-12; (b) triethanolamine; (c) pyridine; (d) aniline; and (e) either of (a)–(e) after introduction of CO_2.

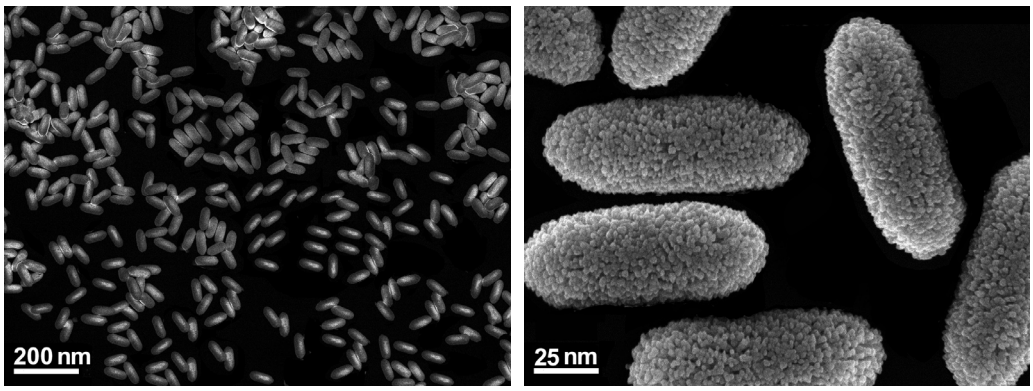

(a) (b)

Fig.S14 STEM images of the as-prepared mesoporous amorphous FeOF nanococoons prepared via SPP with NH_3 and CO_2.

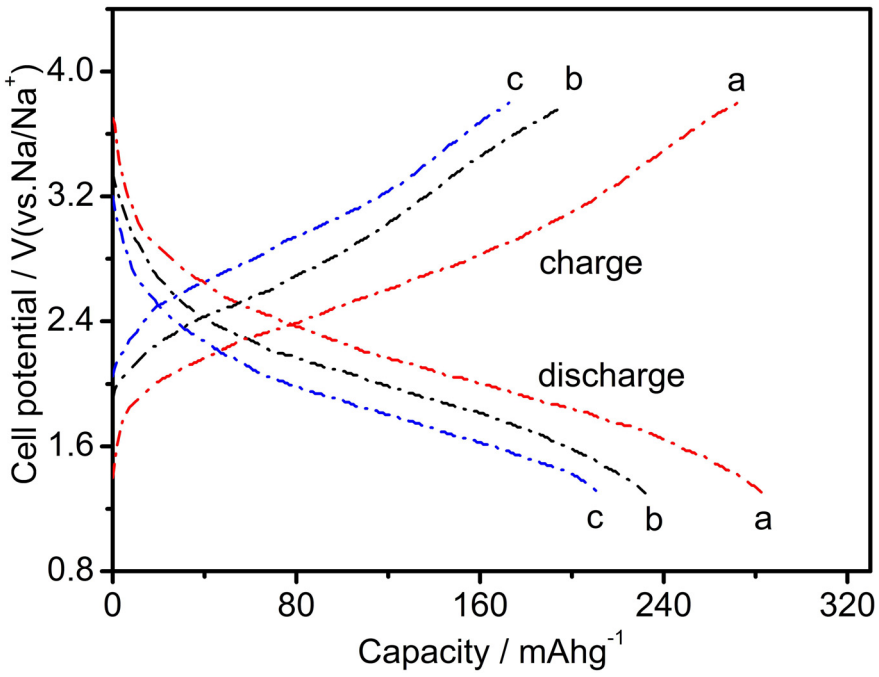

Fig.S15 Initial discharge/charge curves of the as-prepared mesoporous amorphous FeOF nanococoons at the current density of 0.2 Ag^{-1} in different electolytes (a) NaTFSA/TGM, (b)NaTFSA/EC-DEC and (c)NaTFSA/PC.

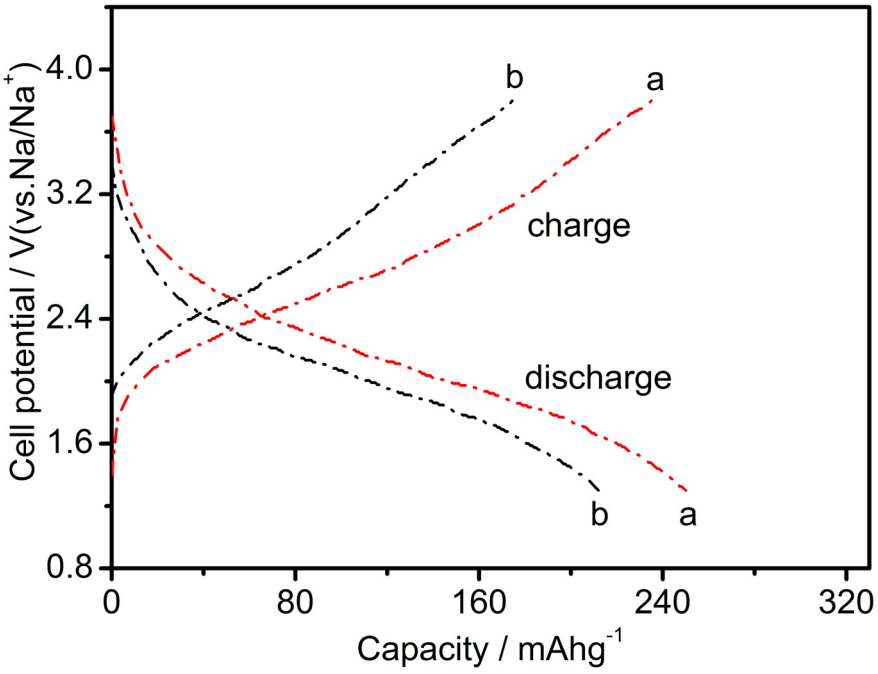

Fig.S16 Initial discharge/charge curves of the as-prepared mesoporous amorphous FeOF nanococoons at the current density of 0.2 Ag^{-1} in different electolytes (a) $NaPF_6$/TGM and (b)$NaPF_6$/EC-DEC.

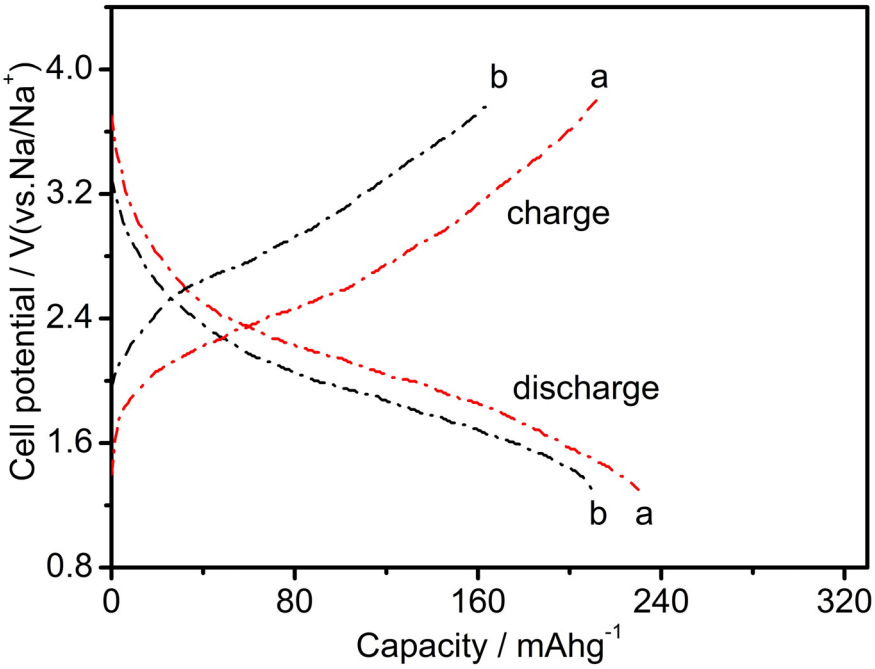

Fig.S17 Initial Discharge/charge curves of the as-prepared mesoporous amorphous FeOF nanococoons at the current density of 0.2 Ag^{-1} in different electolytes (a) $NaClO_4$/TGM and (b) $NaClO_4$/PC.

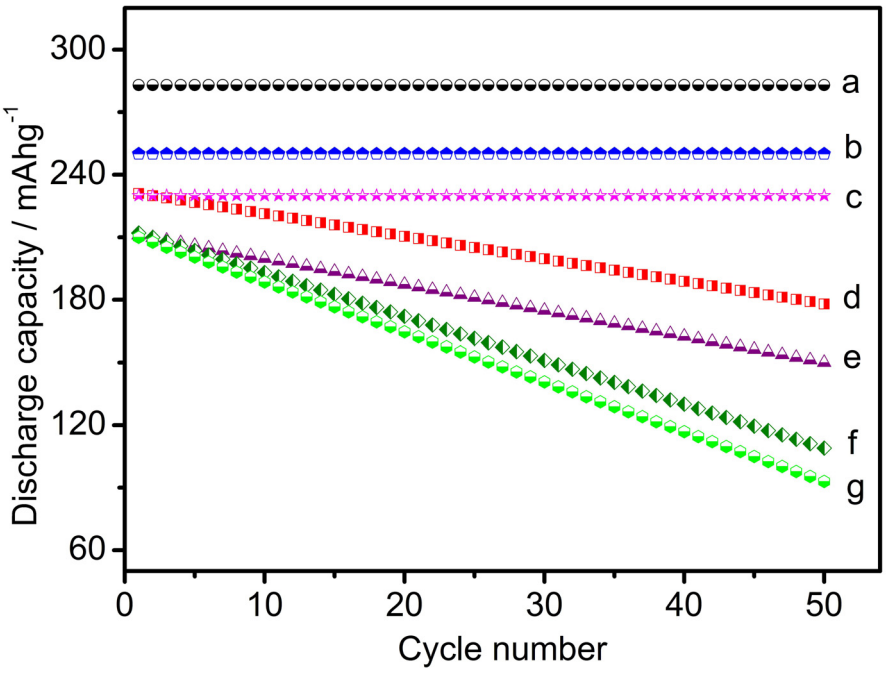

Fig.S18 Cyclability of the as-prepared mesoporous amorphous FeOF nanococoons at the current density of 0.2 Ag^{-1} in different electolytes: (a) NaTFSA/TGM, (b) $NaPF_6$/TGM, (c) $NaClO_4$/TGM, (d) NaTFSA/EC-DEC, (e) NaTFSA/PC, (f)$NaPF_6$/EC-DEC and (g) $NaClO_4$/PC.

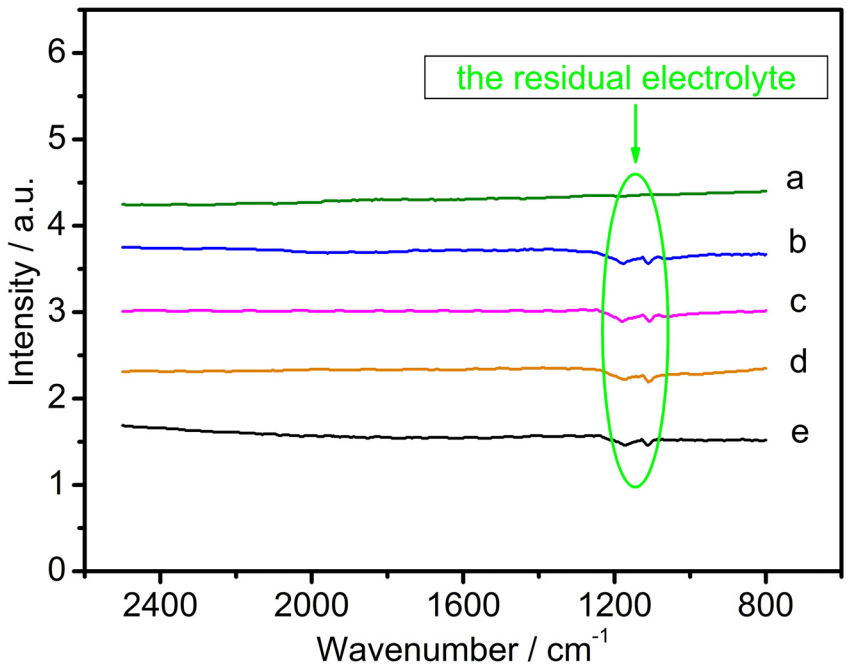

Fig.S19 Typical FTIR spectra of the as-prepared mesoporous amorphous FeOF nanococoons with TGM-based electrolytes charged at different potentials after 10 cycles: (a) 0 V; (b) 2.3 V; (c) 2.8 V; (d) 3.3 V; (e) 3.8 V.

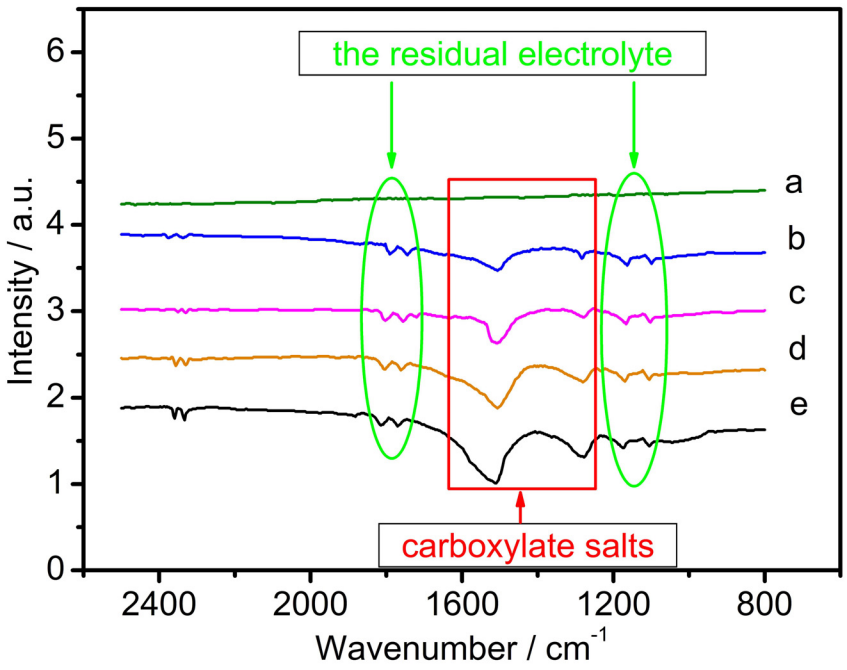

Fig.S20 Typical FTIR spectra of the as-prepared mesoporous amorphous FeOF nanococoons with EC and DEC-based electrolytes charged at different potentials after 10 cycles: (a) 0 V; (b) 2.3 V; (c) 2.8 V; (d) 3.3 V; (e) 3.8 V.

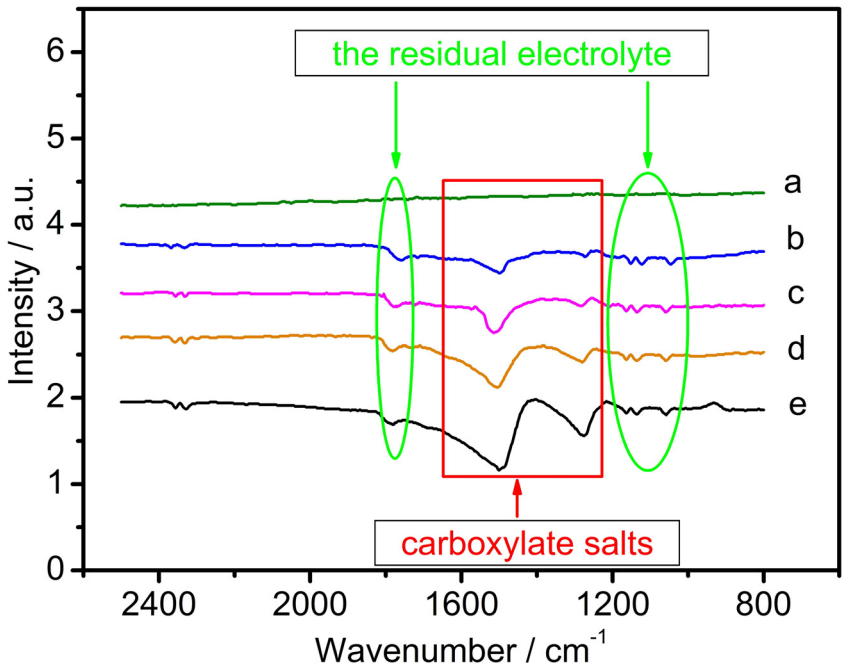

Fig.S21 Typical FTIR spectra of the as-prepared mesoporous amorphous FeOF nanococoons with PC-based electrolytes charged at different potentials after 10 cycles: (a) 0 V; (b) 2.3 V; (c) 2.8 V; (d) 3.3 V; (e) 3.8 V.

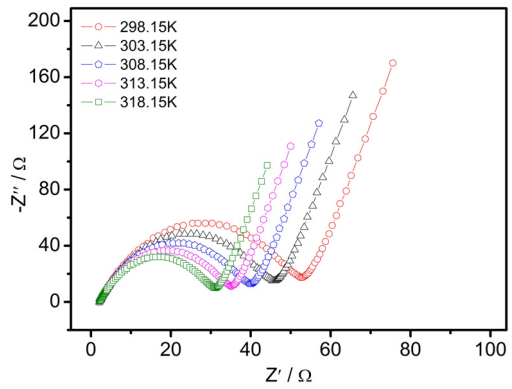

(a)

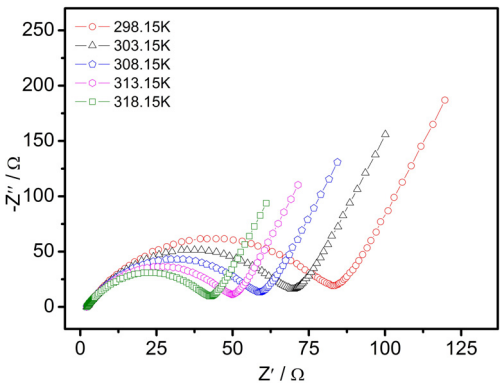

(b)

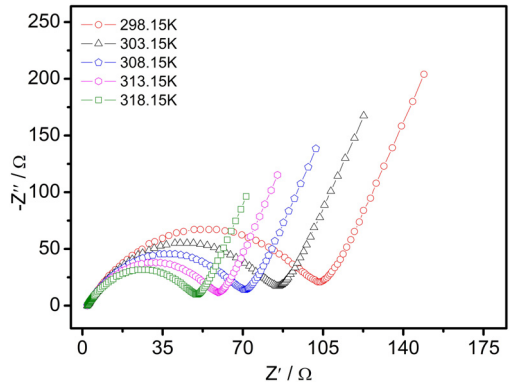

(c)

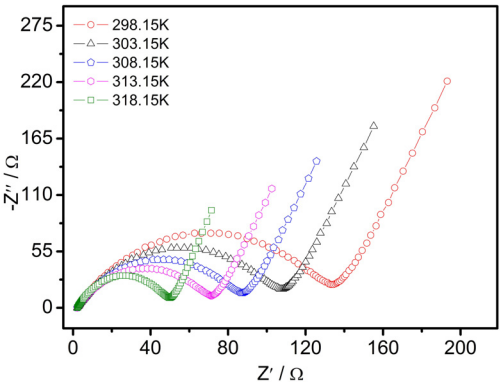

(d)

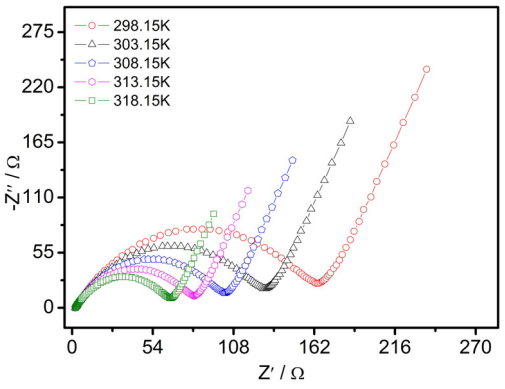

(e)

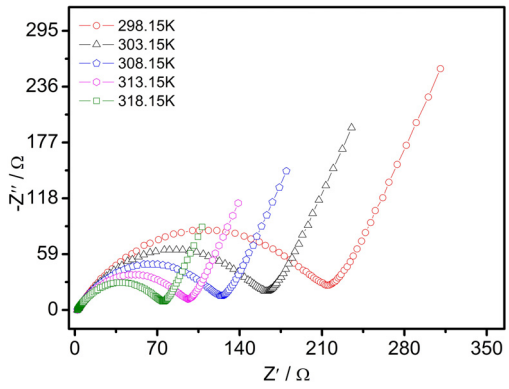

(f)

(Continued)

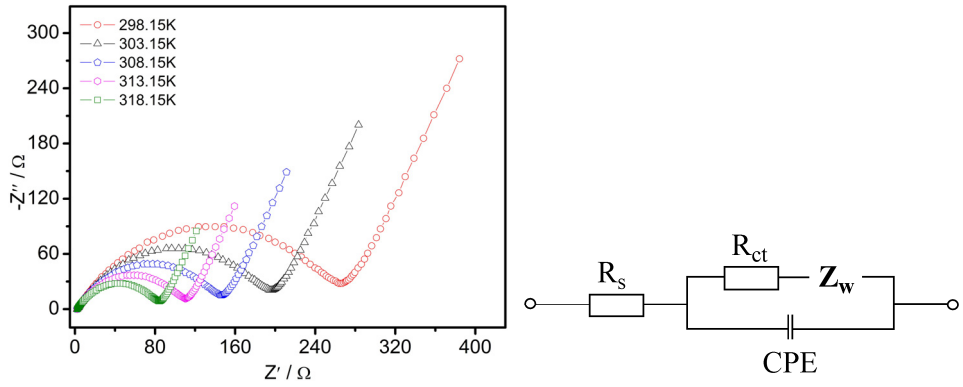

(g) (h)

Fig.S22 Nyquist plots for the as-prepared mesoporous amorphous FeOF nanococoons in different electolytes (a) NaTFSA/TGM, (b) $NaPF_6$/TGM, (c) $NaClO_4$/TGM, (d) NaTFSA/EC-DEC, (e) NaTFSA/PC, (f) $NaPF_6$/EC-DEC and (g) $NaClO_4$/PC obtained by electrochemical impedance spectroscopy (EIS) tests at fully charged states at the 20th charging process. Note: the inserted figure in (h) is the equivalent circuit. Prior to EIS measurement, the as-assembled cells were discharged to 2.8 V and held for 4 h to reach the equilibrium state at different temperatures.

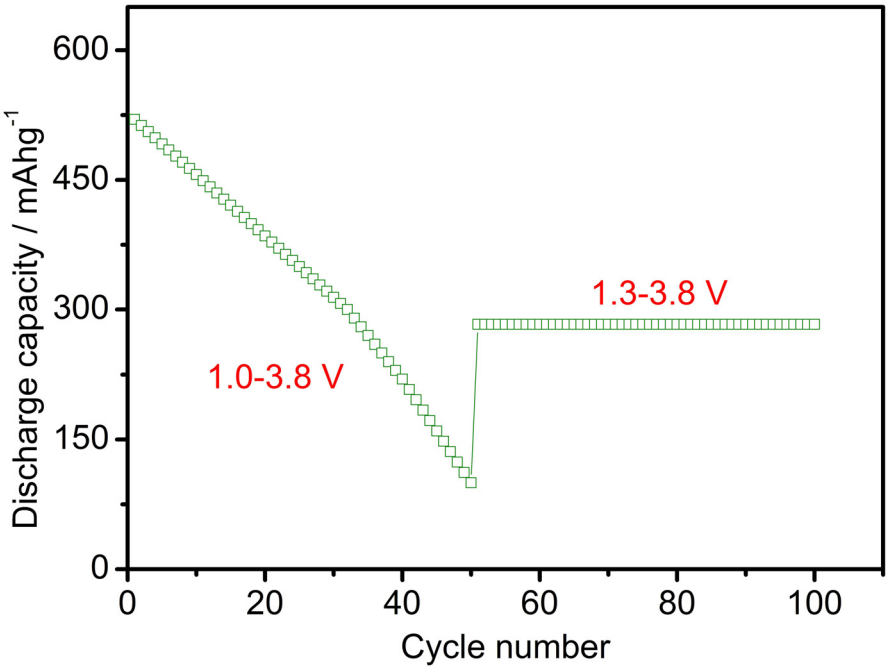

Fig.S23 Cyclic property of the as-prepared mesoporous amorphous FeOF nanococoons in 1.0 M NaTFSA/TGM in the different voltage range at 0.2 Ag^{-1}.

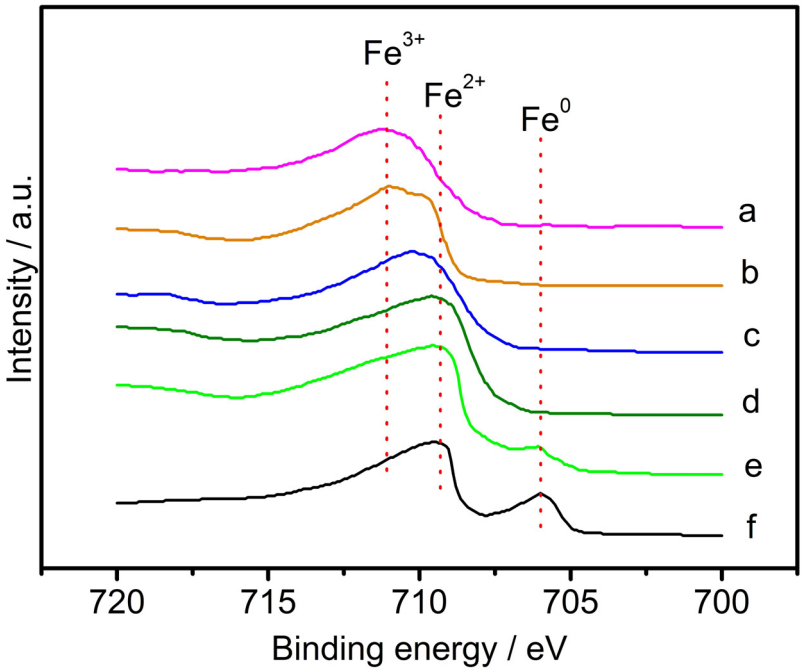

Fig.S24 The typical in-situ Fe $2p_{3/2}$ XPS spectra of the as-prepared mesoporous amorphous FeOF nanococoons TGM-based electrolytes discharged to different potentials at first cycle: (a) before cycling; (b) 3.2 V; (c) 2.2 V; (d) 1.2 V; (e) 1.0 V and (f) 0.7 V.

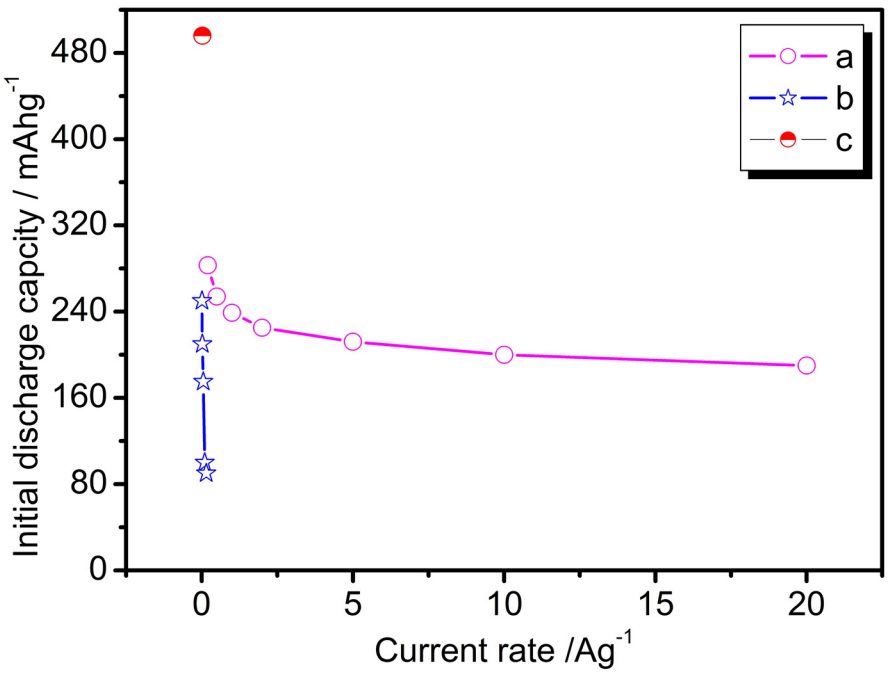

Fig.S25 Rate performance comparison of the samples (a) mesoporous amorphous FeOF nanococoons in this work; (b) FeOF nanorods in Ref. 4; (c) $FeO_{0.7}F_{1.3}$/C in Ref. 5.

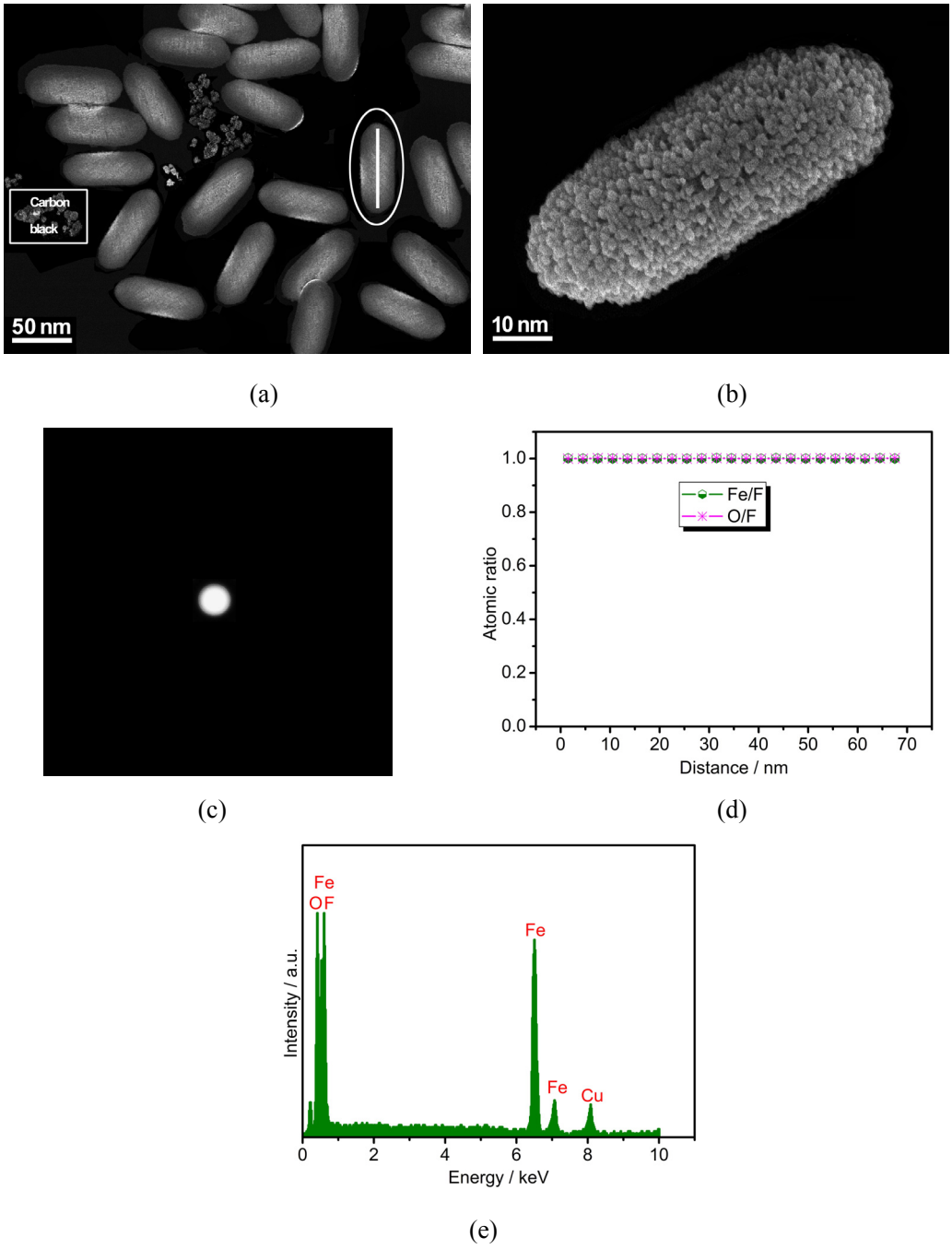

Fig.S26 (a) The high-angle annular dark-field scanning transmission electron microscopy (HAADF-STEM); (b) the enlarged STEM image; (c) SAED pattern; (d) Fe/F and O/F atomic ratios recorded along the white cross-sectional compositional line shown in (a); and (e) EDAX pattern of the as-prepared mesoporous amorphous FeOF nanococoons after cycling at $20Ag^{-1}$ for 1000 cycles. The small nanoparticles observed in the image (a) are carbon black.

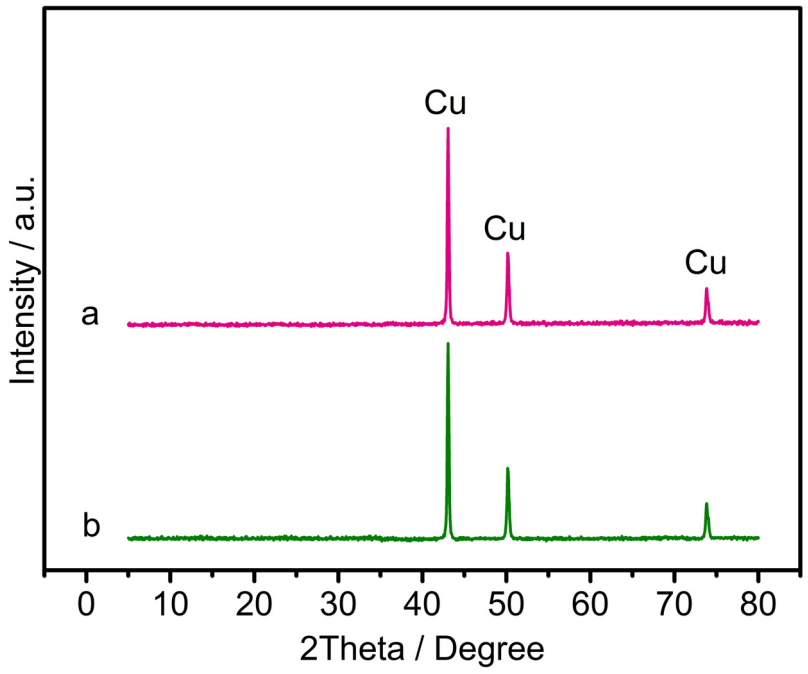

Fig.S27 The XRD patterns of the as-prepared mesoporous amorphous FeOF nanococoons at full charging and discharging states after 1000 cycles. No crystalline peak appears throughout the whole discharging/charging processes expect for the Cu current collector.

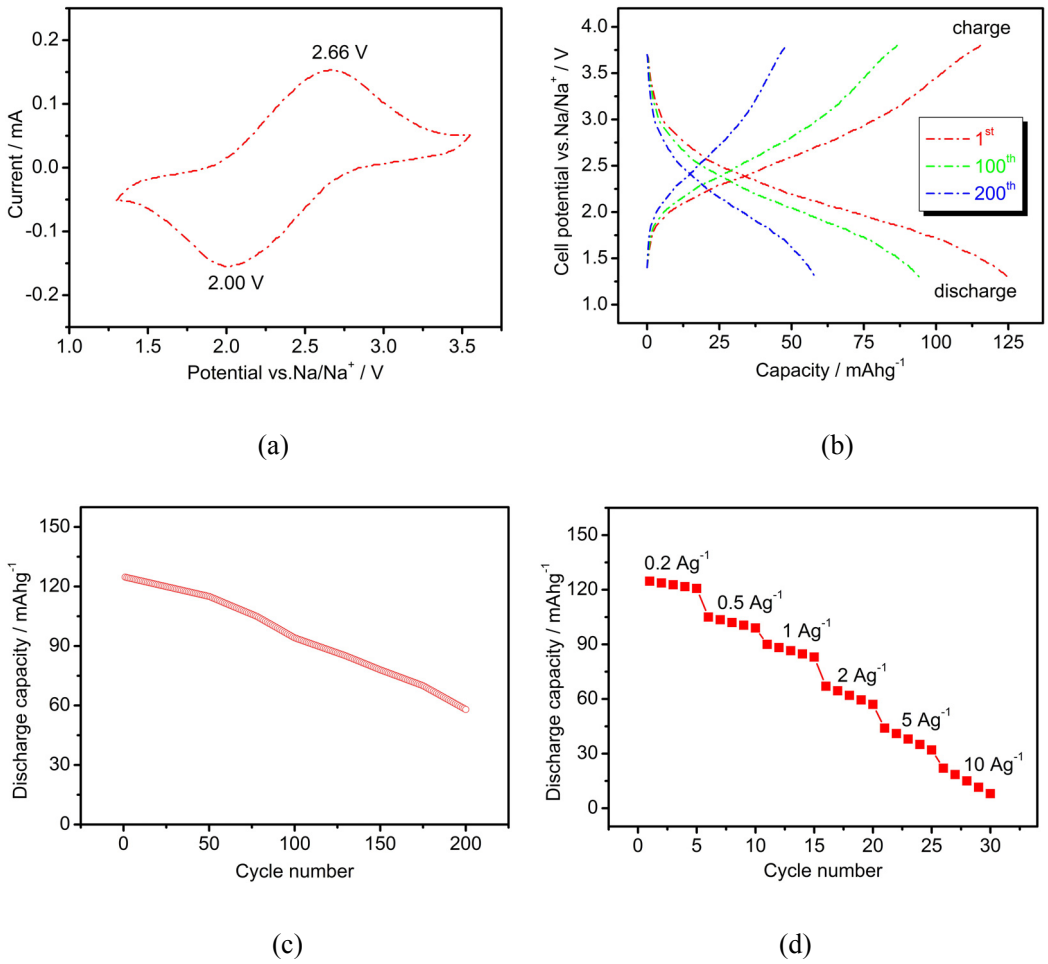

Fig.S28 Electrochemical characterization of the conventional amorphous FeOF: (a) CV curve conducted at a scan rate of 0.1 mVs^{-1} (voltage window 1.3−3.55 V); (b,c) galvanostatic discharging/charging profiles performed at a current density of 0.2 Ag^{-1} and the corresponding cycling performance; and (d) rate capability. The counter electrode was a Na disk and the electrolyte was 1.0 M NaTFSA dissolved in a TGM solution, voltage window was 1.3−3.8 V.

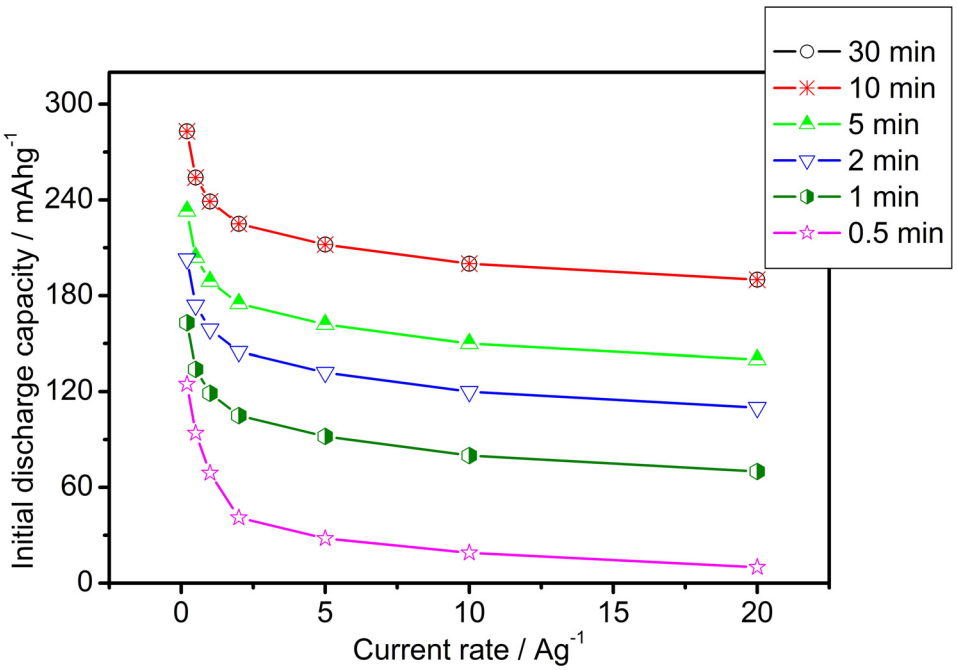

Fig.S29 Rate performance comparison of amorphous FeOF obtained in our work after SPP for different times.